JOURNAL OF MATERIALS SCIENCE 30 (1995) 5589–5599

Induction plasma synthesis of ultrafine SiC powders from silicon and CH_4

J. Y. GUO, F. GITZHOFER, M. I. BOULOS
Plasma Technology Research Center, Department of Chemical Engineering, University of Sherbrooke, Sherbrooke, Quebec J1K 2R1, Canada

Ultrafine SiC powders have been synthesized from elemental silicon and methane using induction plasma technology. The powder products were characterized by X-ray diffraction, thermogravimetric analysis, scanning and transmission electron microscopy, electron probe microanalysis, infrared spectroscopy, and surface area measurement. The powders collected from various sections of the reactor system showed different features reflecting different compositions and powder morphologies. The purest SiC powder was collected in the metallic filter. It was composed of both α- and β-phase of SiC with small levels of free silicon and carbon. The reaction route used is based on the evaporation of the injected pure silicon starting powder, followed by carburization of the silicon vapour using methane. The silicon evaporation rate was found to depend strongly on the particle size of the silicon powder. Using silicon powder with a mean particle diameter of 100 μm, at a plasma power level of $P = 43.2$ kW, the conversion of silicon to SiC and the overall SiC content in the product powder was 44.2% and 50.8 wt%, respectively. The injection probe position was $Z = 9.3$ cm, the silicon feed rate was 4 g min^{-1}, and the C/Si molar ratio was 0.7. Using silicon particles with a mean diameter of 45 μm, the conversion and overall content of SiC increased to 70.4% and 73.9 wt%, respectively, under the same plasma operating conditions and powder feed rates. By appropriate selection of experimental conditions, ultrafine SiC powder of high quality was achieved.

1. Introduction

SiC is one of the most important ceramic materials. Owing to its high strength, high abrasion resistance, electrical conductivity, high thermal conductivity and good high-temperature chemical stability, it has a wide range of applications as a high-temperature structural material. Sintered silicon carbide turbine blades, diesel engine parts and components for nuclear reactors are some typical examples where these properties are important. Over the past decade a great variety of processes have been proposed for the preparation of SiC powders of high purity, ultrafine particle size and good dispersion. These were mostly based on the use of readily vaporized starting materials, such as SiH_4 [1–5], CH_3SiCl_3 [6, 7], $Si(CH_3)_4$ [8] and $SiCl_4$ [9–12] because of their favourable thermodynamics and the ability to produce ultrafine and uniform-sized particles by homogeneous nucleation and growth from the gaseous phase. The problem with such process routes is their high production cost because the precursors are normally expensive, and many of them are corrosive and/or toxic, contributing to difficulties in handling of the materials. In certain cases, chloride-ion contamination of the powder products is unavoidable, which has a detrimental effect on the sintering properties of the powders and the mechanical properties of the sintered body [13]. Ultrafine SiC powder has also been produced from SiO_2 and silicon as starting materials [14–16]. The purity of the powders obtained by these methods was not satisfactory for achieving high densification.

Plasma technology is one of the leading techniques for the production of high-purity ultrafine metal and ceramic powders. Both d.c. arc plasma and r.f. induction plasmas have been used to prepare SiC powders, mainly through the use of silane or organosilanes as the precursor. A few studies have also been reported on the preparation of SiC powders with solid precursors using plasma technology. Ando *et al.* [17] prepared SiC powder by evaporating a silicon ingot used as an anode in a CH_4 transferred arc system. A carbon rod was used as the cathode in this case. Kong *et al.* [18, 19] reported the synthesis of SiC in a d.c. thermal plasma using SiO_2 or laboratory-produced SiO and CH_4 as starting materials. They obtained a mixture of α- and β-SiC, though with significant amounts of additional by-products such as SiO, free silicon, free carbon and unreacted SiO_2. Tanaka *et al.* [20–22] systematically investigated the preparation of ultrafine SiC and Si_3N_4 starting with silicon bulk material using a transferred-arc plasma reactor.

The present study was undertaken to explore the synthesis of high-purity ultrafine SiC powder through the use of particulate metallic silicon and methane as

0022–2461

the starting materials in an r.f. induction plasma reactor. The properties of the powders collected from different parts of the reactor system were subjected to extensive analysis. Quantitative phase composition was determined by X-ray diffraction (XRD), combined with thermogravimetric analysis (TGA).

2. Thermodynamic investigation

Thermodynamic investigation provides general guidelines for the expected reactions and species that may be formed at different temperatures. Thermodynamic calculations for the Si–CH_4–Ar–N_2 system were performed using a Gibb's free-energy minimization program developed at the University of Sherbrooke. These calculations provide equilibrium concentrations for different reaction species at various temperatures. The overall reaction for SiC formation may be written as follows

$$Si(s) + CH_4(g) = SiC(s) + 2H_2(g) \quad (1)$$

The calculation results for various molar ratios of Si/CH_4 are shown in Figs 1–3. When silicon is exposed to nitrogen plasma, it combines with nitrogen to form $Si_3N_4(s)$, which decomposes at temperatures above 2000 K. With CH_4 present in the system, the main species generated at temperatures above 3000 K

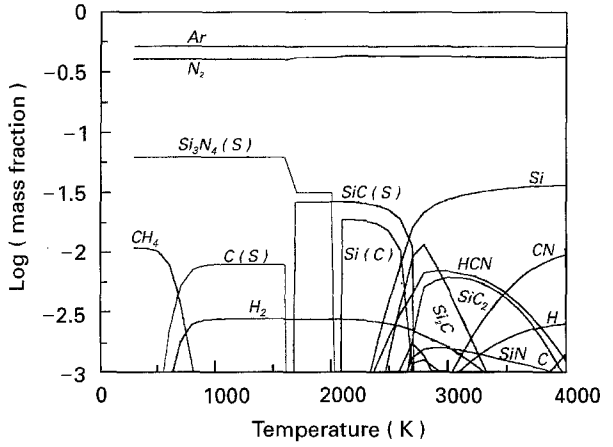

Figure 1 Thermodynamic equilibrium diagram for the system $Si:CH_4:Ar:N_2 = 1.0:0.5:9.5:11.5$.

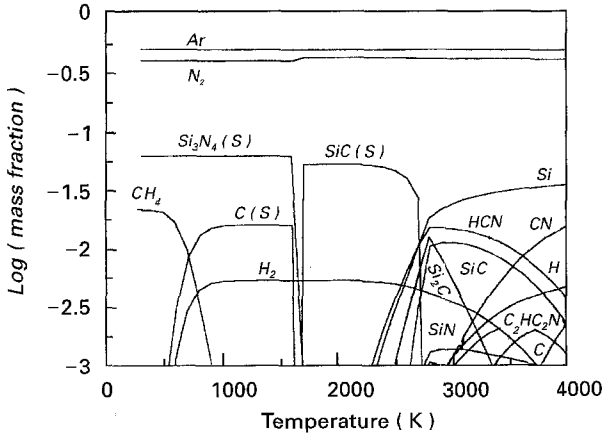

Figure 2 Thermodynamic equilibrium diagram for the system $Si:CH_4:Ar:N_2 = 1.0:1.0:9.5:11.5$.

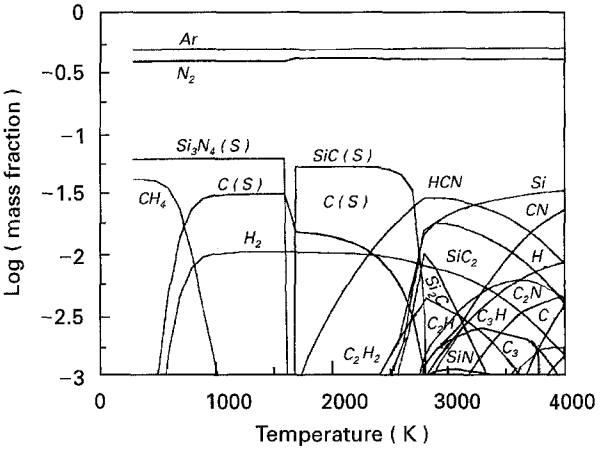

Figure 3 Thermodynamic equilibrium diagram for the system $Si:CH_4:Ar:N_2 = 1.0:2.0:9.5:11.5$.

are HCN(g), Si(g), SiC_2(g), Si_2C(g), H_2(g), H(g), C_2H_2(g), C_2H(g), C_3H(g), CN(g), C_2N(g), C_3(g), C(g), N_2(g) and Ar(g). From the thermodynamic viewpoint, the highest potential for the SiC formation lies in the temperature range 1700–2800 K. It is noteworthy that in this range the other main species present include H_2(g), Si(s), C(s) and HCN(g) depending on the molar ratios of Si/CH_4. From the equilibrium diagram it may be seen that the products of methane decomposition vary with temperature: from 500–1750 K they are solely C(s) and H_2(g); from 1750–2400 K they are C(s), H_2(g), HCN(g); and at over 2400 K, C_2H_2(g), C_2H(g), C_3H(g), H(g), and others are generated successively.

3. Experimental procedure

The starting material used principally in this study was metallic silicon powder (Cerac Corp.), with a chemical purity better than 99 wt % Si. Two powders, with mean particle size of 100 μm (designated Si-100) and 45 μm (designated as Si-45), respectively, were used in the experiments. The main impurities in the starting powder detected by electron probe microanalysis (EPMA) were iron, aluminium, calcium, copper, molybdenium and titanium. The Tekna PL-50 r.f. plasma reactor system used for the synthesis of SiC is shown in Fig. 4. The system is composed of a plasma torch, a cylindrical stainless steel reactor, a cyclone, a metallic filter, and an exhaust evacuation.

The metallic silicon powder was oven-dried and loaded into a powder feeder (Sylvester Company, Mark IX). Both the silicon powder and the methane were introduced into the plasma by means of a water-cooled stainless steel probe. The position of the probe could be adjusted vertically.

Before each test, the reactor system was twice evacuated to about 25 torr with intermediate argon flushing to purge air. The r.f. plasma was initiated with industrial grade argon supplied at 25–50 torr. Hi-dry nitrogen was then introduced to produce the desired plasma gas mixture. Under required conditions of constant plate current and plate voltage, methane and metallic silicon powder were simultaneously fed into the plasma. The CH_4 flow rate was measured by

a rotameter, in units of standard litres per minute (sl min^{-1}). The feed rate of silicon powder was controlled by setting the rotation speed of the feed screw of the powder feeder, which had been previously calibrated by observing weights of delivered powders for given feeder operation periods (g min^{-1}). Experiments were generally conducted under pressures slightly lower than atmospheric and silicon powder feed runs were varied from 5–10 min. Operating conditions employed in the SiC powder synthesis are summarized in Table I.

The synthesized SiC powder was collected by means of two sintered metal filters and its structure and composition were analysed using an X-ray diffractometer (Rigaku Geigerflex) with CuK_α radiation at a scanning rate of 2° min^{-1} with the following slit settings DS = 1.0°, RS = 0.3°, and SS = 1.0°. The acquisition range was normally from 20°–50° for 2θ because all the desired information was presented in this range. The free carbon content in the powder was determined by thermogravimetric analysis (TGA) in an oxidizing atmosphere (air). The heating rate used was 2.5 °C min^{-1} and the maximum temperature was set at 1000 °C. Infrared spectroscopy was used to assess the presence of Si–O bonded species in the powder with KBr used as matrix material. Electron probe microanalysis attached to the SEM was also employed to detect the presence of oxygen and metallic impurities originating from the source materials. The microstructure and particle shape and sizes of the powder were monitored by electron microscopy (Jeol JSM 840 A SEM and Philips EM 300 TEM). The surface area of the powder was measured by the BET method (Micromeritic Flowsorb II 2300 BET), using nitrogen as adsorbate.

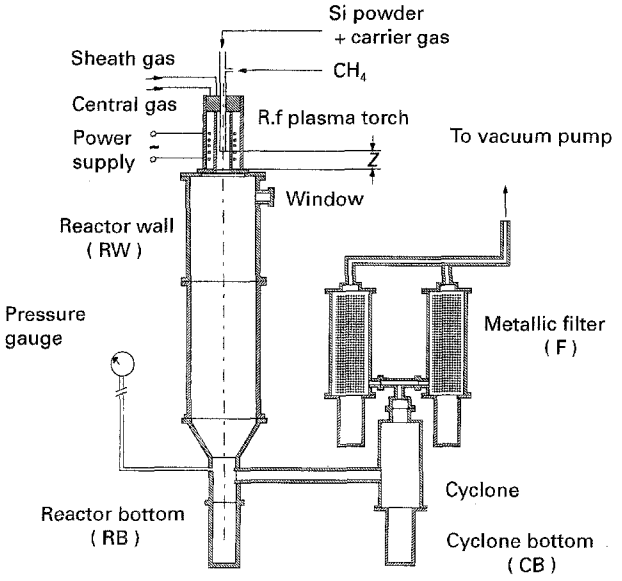

Figure 4 Schematic drawing of the experimental apparatus for synthesis of ultrafine SiC powder.

4. Results and discussion

Thermodynamically, the reaction, $Si(s,l) + CH_4 \rightarrow SiC(s) + 2H_2$ can take place over a wide range of temperatures (300–2700 K) [23] if no other reactive gas is involved. Under a nitrogen atmosphere, SiC formation occurs in the range 1700–2800 K, as described previously. However, the extent of reaction is determined by the diffusion mechanism from gas to solid or from gas to liquid or by solution–precipitation which requires fairly long periods to complete. Moreover, chemical reactions occurring between gas and solid or gas and liquid or liquid and solid do not normally result in the formation of ultrafine particles. The approach adopted in the present study was therefore based on the gas phase reaction in order to prepare ultrafine powders by plasma.

4.1. Evaporation of metallic silicon particles and the decomposition of methane

As a first experimental step, the melting and evaporation of silicon particles in the plasma was examined. The boiling point of silicon is relatively high and thus in-flight evaporation of silicon is relatively difficult. A few preliminary tests were conducted on the injection and in-flight evaporation of metallic silicon particles. The ranges of operational conditions for performing these tests were as follows: plate power level, 30–35 kW; plasma gas, Ar + N_2; reactor pressure, ~ 500 torr; Si (Si-100) powder feed rate 3.63–5.64 g min^{-1}; feed time, 5 min. The powder obtained appeared yellow–brown in colour. Fig. 5 shows a transmission electron photograph of the silicon powders collected in the filters. It is seen that the particle sizes of filter-collected powders were basically in the range 0.1–0.4 μm, confirming the evaporation and condensation mechanism of the injected silicon particles in the plasma. X-ray diffraction (XRD) of the powder shows only the pattern peaks characteristic for silicon. However, in Fig. 5, some fibre-shaped particles are also observed surrounding silicon particles

TABLE I Summary of the operation conditions used for the synthesis of SiC powders

Run	Si mean particle size (μm)	Powder carrier gas	Plate power level (kW)	Probe position, z (cm)	Reactants feed rate		C/Si molar ratio	Feed time (min)
					Si (g min^{-1})	CH_4 (sl min^{-1})		
1	100	Ar	43.2	9.3	3.89	2.5	0.74	6
5	100	Ar	40.0	7.2	2.18	1.3	0.68	10
S2	45	Ar	41.3	8.0	4.35	2.5	0.66	5
S8	45	Ar	52.2	8.0	2.15	3.2	1.70	5
S15	45	CH_4	52.2	8.0	2.03	3.8	2.14	5

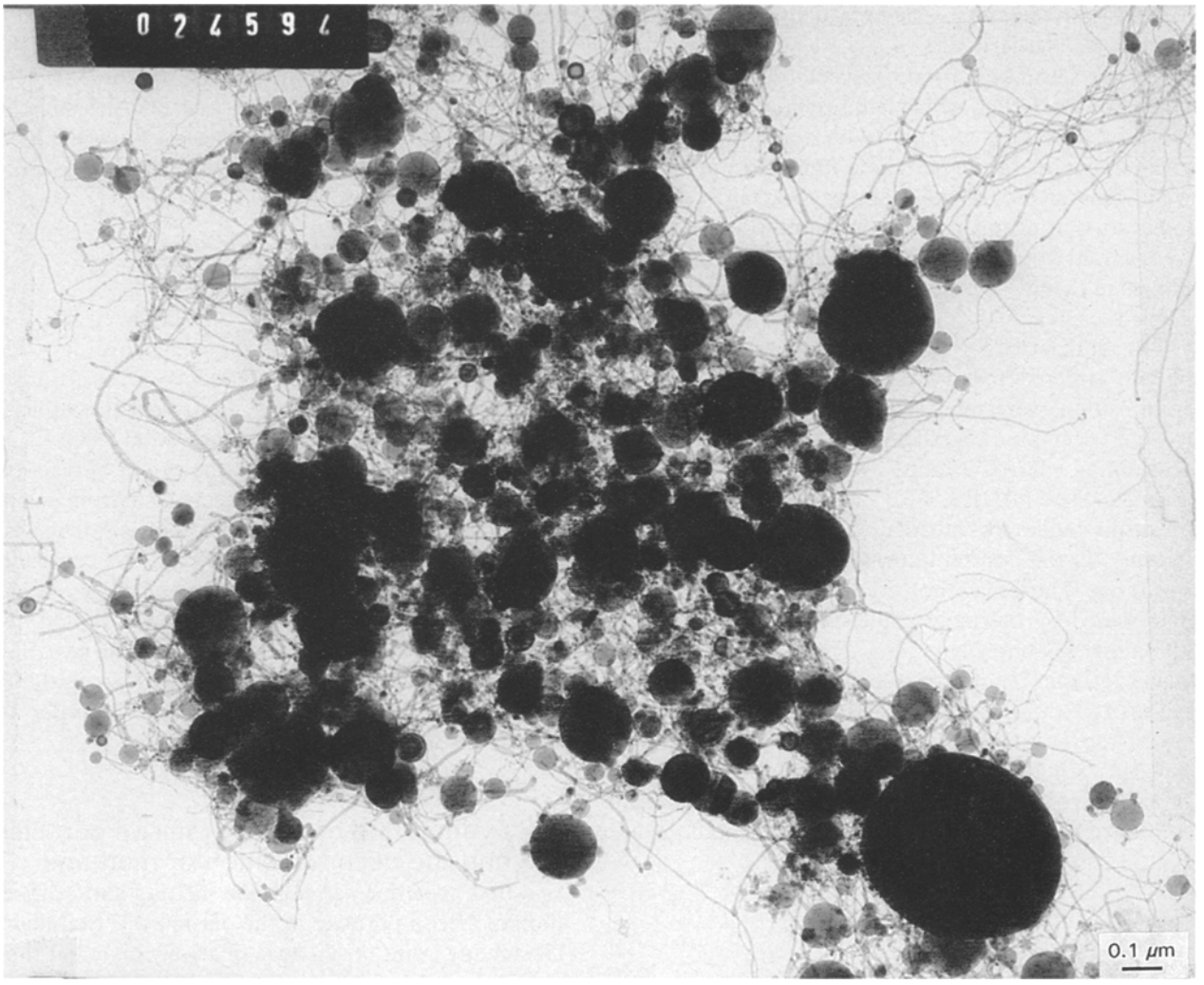

Figure 5 Transmission electron micrograph of plasma-evaporated silicon powder (Sample RFSi-1) showing the evaporation of silicon and the occurrence of "SiO".

under TEM analysis. These can be attributed to "SiO" condensates [24], formed and quenched as a metastable phase during the evaporation–recondensation process. The formation of "SiO" can be attributed to the presence of a low residual oxygen partial pressure in the plasma gas and reactor system.

It should be pointed out that the Si-100 silicon particles, injected at the rate of 3.63–5.64 g min^{-1}, are not completely evaporated because of their large size, even with the relatively long residence time characteristic of r.f. plasmas. Proulx *et al.* [25, 26] showed that the vapour cloud, generated by vaporization and evaporation which surround the particle, greatly affecting the heat-transfer rates between the plasma and the particle. In the present case, the evaporated portion was estimated to be around 25–35 wt % for these circumstances, i.e. the average evaporation rate was 1.2–1.4 g min^{-1}. Precise determination of the evaporation rate is experimentally difficult. The presented data are proposed, based on both the silicon product powder collected in the filter and the conversion of silicon to SiC in the subsequent synthesis tests with the assumption that the filter collected powder was the evaporated silicon, and that the evaporated silicon would be completely converted to SiC. Unevaporated or incompletely evaporated particles are mainly deposited on the reactor wall or bottom, particularly the larger particles.

Decomposition tests for CH_4 were also carried out to verify the formation of carbon and to identify the particle size and shape of the free carbon. The plasma operating conditions were similar to those for the silicon evaporation tests. CH_4 was injected through the central probe into (Ar + N_2) plasma at a feed rate of 2.5 sl min^{-1}. The obtained carbon product was very fine in size and had a very good flowability. Owing to the difficulty in collection of all the produced carbon powder, the portion of CH_4 decomposed to carbon could not be precisely determined. Thermodynamically, CH_4 starts to dissociate to C(s) and H_2(g) at temperatures below 1000 K. As the temperature is increased to > 1750 K, some C(s) reacts with nitrogen and hydrogen to form HCN(g). As the temperature is further increased to > 2400 K, more carbon-containing gaseous species are generated, whereas C(s) is reduced drastically and disappears totally above 2800 K. Therefore, it can be inferred that the decomposition of CH_4(g) to C(s) in the plasma is incomplete.

Fig. 6 shows a transmission electron micrograph of the free carbon powder obtained by CH_4 decomposition. It may be seen that the particles are nearly

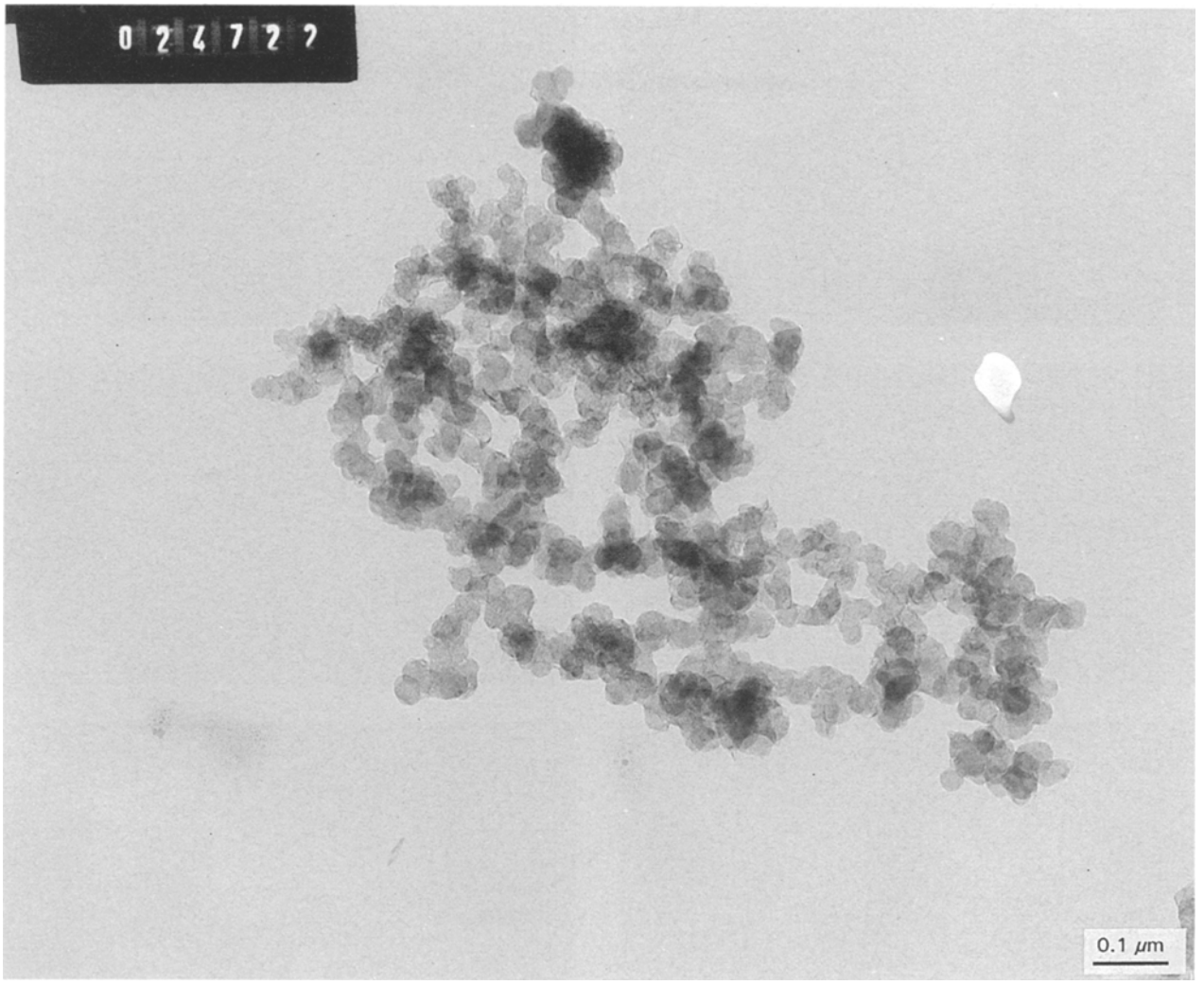

Figure 6 Transmission electron micrograph of free carbon produced by decomposition of CH_4.

spherical, with average particle sizes in the range of 10–30 nm.

4.2. Synthesis of SiC from injected silicon and CH_4

Synthesis experiments were performed with the methane used as the carburizing agent, based on the preliminary evaporation tests of metallic silicon particle. Table I lists the variable parameters for five reaction runs including plate power level, probe position, powder carrier gas, feed rate and C/Si molar ratio and particle size of the starting silicon powder. Plate power level was set at generally higher levels than was the case for the pure silicon evaporation tests. This was because much greater heat energy is required when silicon powder and CH_4 are injected into the plasma simultaneously. Decomposition of CH_4 is endothermic. To compensate for the energy losses and to ensure a certain rate of evaporation of silicon, increased plasma power levels were necessary. Probe position has an important effect on the evaporation and synthesis processes. The distance Z represents the degree of deviation of the probe exit from the core of the plasma fireball. The plasma becomes increasingly sensitive to the position of the probe as it approaches the plasma core, which therefore limits the available range of the probe position. Feed rates and the C/Si molar ratio in the injected starting materials significantly affect the compositions of the produced powders. The variation range of the silicon feed rate was determined basically from the results of the preliminary evaporation tests. The flow rates of CH_4 were selected such that C/Si was non-stoichiometric, ranging from CH_4 deficient to CH_4 excess conditions. Because CH_4 dissociates into a number of carbon-containing species at high temperatures, a certain amount of excess CH_4 was expected to be beneficial for the carburization of silicon. The change of carrier gas was made to examine if it also affects the synthesis.

4.2.1. Powder collection

Synthesis experiments indicated that powders recovered at the alternate collection positions have different physical features and varying chemical compositions. In order to identify and control the powder quality, the powders collected at the different system positions were treated individually. Fig. 7 shows a group of scanning electron micrographs of the powders collected at (a) the reactor bottom, (b) the reactor wall, (c) the cyclone bottom, and (d) the filter,

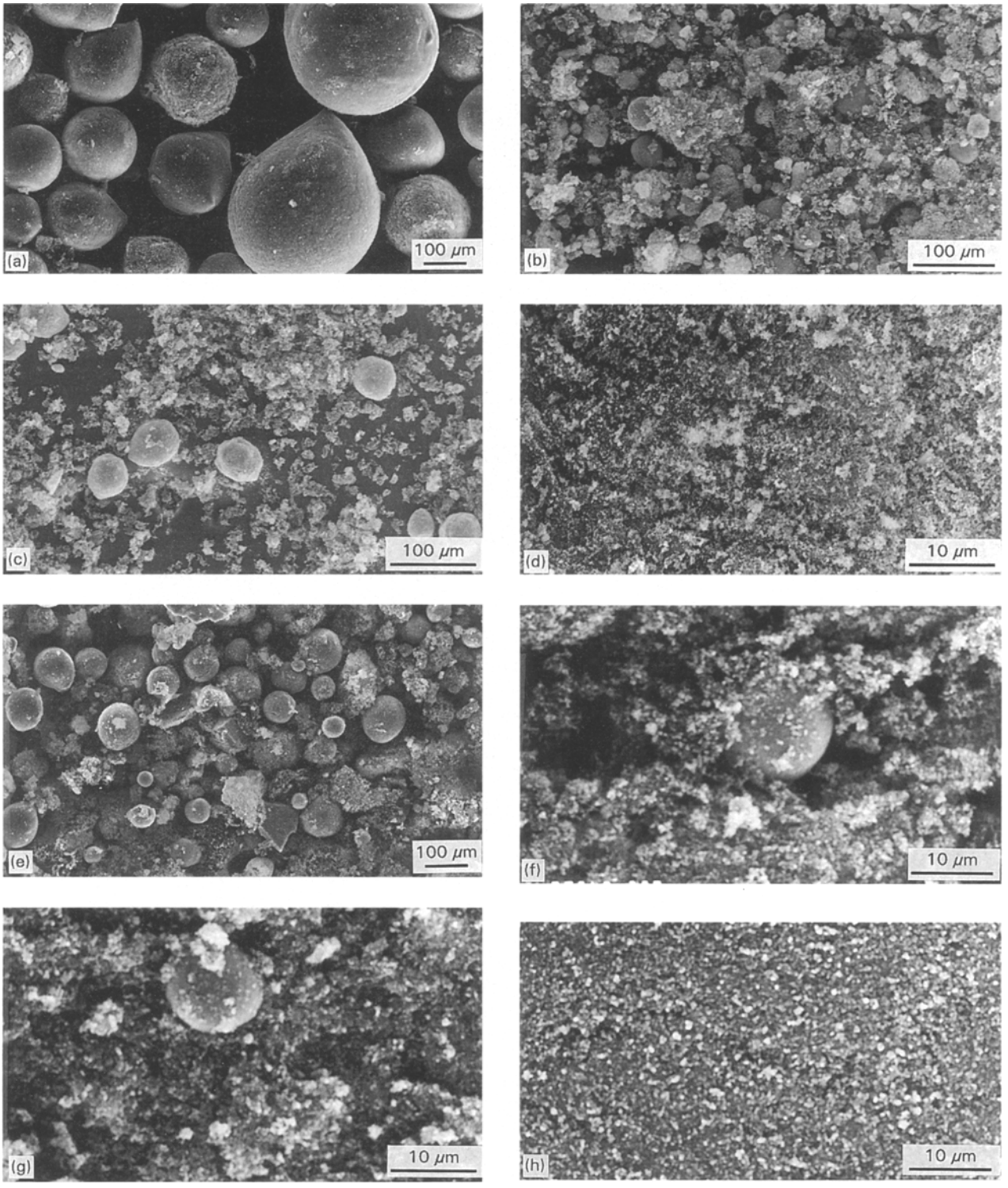

Figure 7 Scanning electron micrographs of the powders collected at different positions in the SiC synthesis, showing the distribution of the melted but unevaporated silicon particles in the different positions. (a–d) Run RFSiC-5; (e–h) Run RFSiC-S8.

respectively. Fig. 7a–d relate to the use of Si-100 as starting material (run RFSiC-5). In this instance, the powder, collected on the water-cooled reactor wall (W_{RW}) was a mixture of unreacted silicon, free carbon and silicon carbide, the unreacted silicon being the dominant component. The powder collected in the reactor bottom (W_{RB}) consisted of almost 100% spheroidized metallic silicon. Powders collected in the two metallic filters (W_F) were nearly pure silicon carbide (both α- and β-SiC), with a little free carbon in some samples. Powder collected in the cyclone (W_{CB}) was also a mixture of unreacted silicon, free carbon and silicon carbide, with a preponderance of free carbon. Figure 7e–h are for the case of Si-45 used as the starting powder (run RFSiC-S8). Pictures of the powders collected at the corresponding positions all show that the same distribution pattern for the different components in the powders holds, but the free silicon contents were considerably reduced. Both reactor wall and cyclone bottom powders contained much less free silicon, and the reactor bottom powder in particular is not pure spheroidized silicon but a mixture of free silicon and other components (SiC, free carbon). Filter powder basically contains pure SiC. Reactor powder

TABLE II Mass balances for the different runs of ultrafine SiC synthesis

Run	Total injected Si powder (g)	Collected powders (g)				Total recovery, W_T (g)
		W_{RW}	W_{RB}	W_{CB}	W_F	
1	23.3	14.8	3.4	4.0	3.3	25.5
5	21.8	14.5	4.6	4.5	3.0	26.6
S2	21.8	16.0	~0	5.6	5.8	27.4
S8	10.7	8.9	~0	2.7	3.4	15.0
S15	10.2	8.2	~0	2.1	3.9	14.2

appeared light grey or grey in colour; filter powders were grey or dark grey and cyclone bottom powders were dark grey or black. The weight percentage of each part of the powder in the total collected powders was W_{RW} 55%–65%, W_{RB} 10%–17%, W_F 11%–13%, and W_{CB} 13%–17%, respectively, for Si-100, and W_{RW} 58%–64%, $W_{RB} \sim 0\%$, W_F 23%–28%, and W_{CB} 11%–18%, respectively, for Si-45. Table II summarizes the mass balances for the different runs listed in Table I.

4.2.2. Powder characterization

Obvious differences among the XRD spectra of the powders, collected at the different positions, were apparent as shown in Fig. 8 for runs S8 and S15. The other samples had similar diffraction patterns. This implies that the reactor system employed has the ability substantially to separate the different components in the powder products, i.e. unevaporated metallic silicon, unreacted free silicon, free carbon, and silicon carbide. The uneven distribution of the various components arises from their different geometric dimensions, as will be seen later.

In Fig. 8, the peaks at 26.0° and 44.8° are characteristic of graphite, whereas those at 28.3° and 47.2° are attributed to metallic silicon. All the remaining peaks, i.e. 34.2°, 35.8°, 38.1°, 41.5°, and 45.4°, belong to silicon carbide phases, among which the peaks at 34.2°, 38.1° and 45.4° are typical of the hexagonal alpha phase of SiC. Obviously, the SiC powder produced is a mixture of the α- and β-phase structures. SiC is polymorphous; there are many polytypes of this phase structure, the most common are the 2H, 4H, 6H and 15R α-SiC. The cubic structure of the beta phase has only one polytype, i.e. 3C β-SiC. In the present study, the powder produced is mainly composed of 3C-SiC and 2H-SiC. As far as the phase composition is concerned, generally, the synthesis tests with Ar + N_2 plasma gas resulted in more β-SiC than α-SiC without exception. The ratio of the β-SiC to α-SiC ranged from 1.2–1.6. However, the situation can be changed when hydrogen is used to replace nitrogen as the plasma gas. The results of these tests are given elsewhere.

In the quantitative evaluation of the phase composition of the powder, only crystalline phases detected were taken into account. The free carbon content was determined by thermogravimetric analysis, it being likely that some amorphous "carbon black" exists in the powder [27]. Typical curves for the TGA analysis shown in Fig. 9 reveal that combustion of the free carbon in air begins at around 530 °C and ends at about 680 °C. Above this temperature, SiC powder is oxidized at an increasing rate. Comparing Fig. 9 with Fig. 8, it is found that the variation trend of free-carbon content, detected by TGA in the powders collected at the various positions, is in accord with that determined by quantitative XRD analysis. The quantitative results of the phase analyses are set out in Table III, which reveals that the SiC content in the filter powders was generally > 95 wt %. The chemical compositions of the reactor powders and cyclone

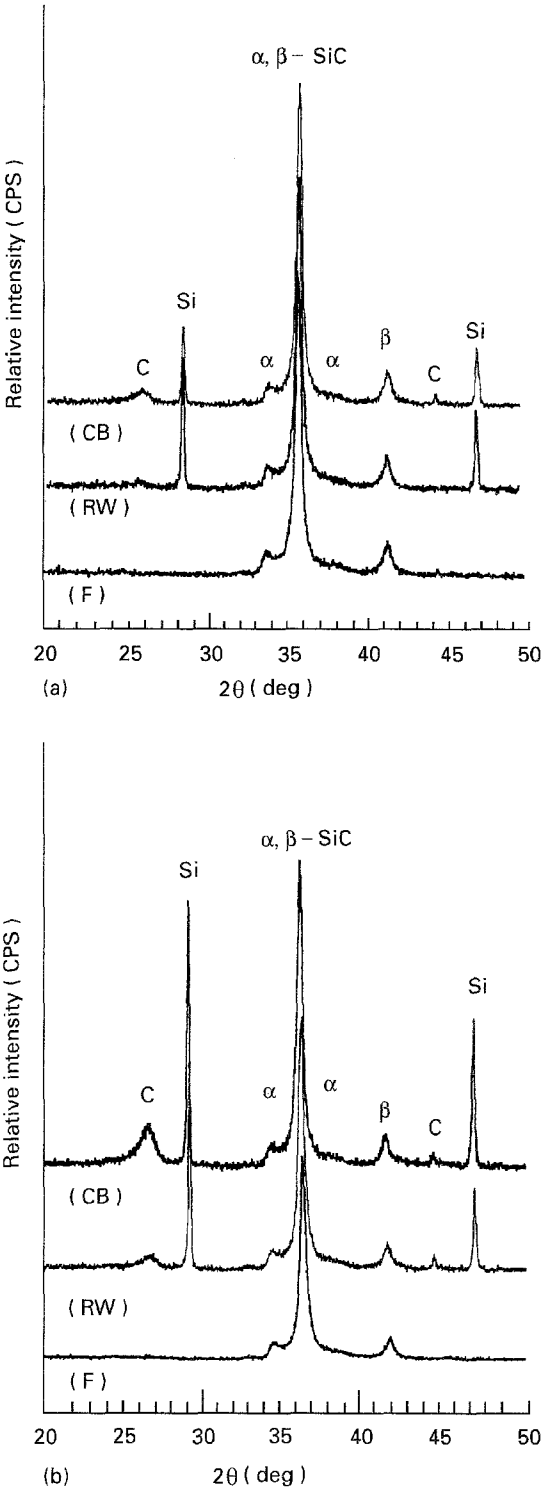

Figure 8 XRD patterns of the powders collected at different positions, showing the differences in chemical composition. (a) Run RFSiC–S15; (b) Run RFS: C–S8.

powders varied with power level, probe position, feed rates and C/Si molar ratios of the starting materials. Typically, SiC contents of these two powders were 50 wt % for Si-100 and 80 wt % for Si-45, respectively.

For calculation of the overall content of SiC in the total powder products and conversion of injected metallic silicon to SiC, the following equations were used

$$SiC_{over} = \frac{SiC_{RW} \times W_{RW} + SiC_{RB} \times W_{RB} + SiC_F \times W_F + SiC_{CB} \times W_{CB}}{W_{RW} + W_{RB} + W_F + W_{CB}} \times 100\% \quad (2)$$

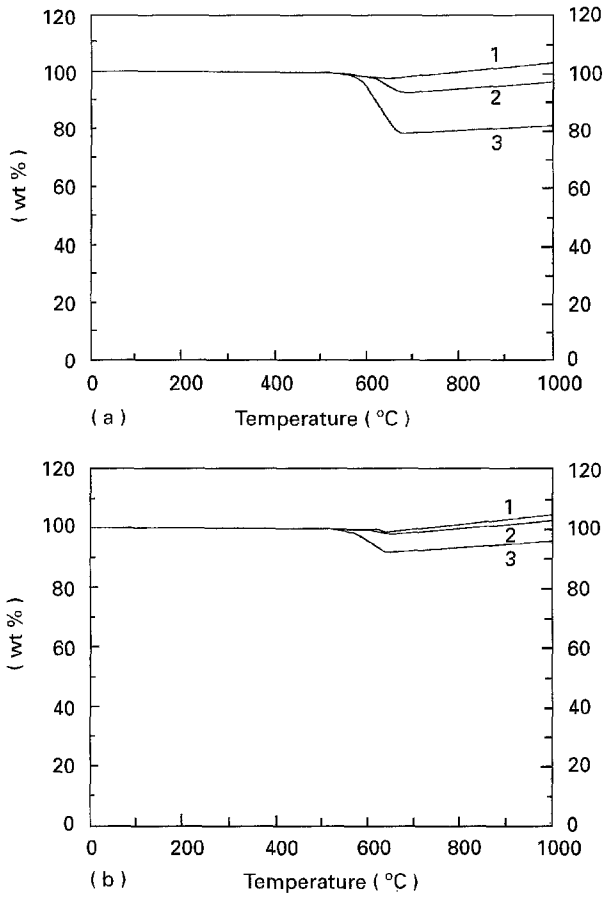

Figure 9 Typical TGA curves of the powders from different collection positions, showing the variation of free carbon content. (a)1, S8F; 2, S8RW; 3, S8CB. (b) 1, S15F; 2, S15RW; 3, S15CB.

$$Si_{conv.} = \frac{Si_{SiC}}{Si_T} \times 100\%$$

$$= \frac{(SiC_{RW} + SiC_{RB} + SiC_F + SiC_{CB}) \times 0.7}{Si_{RW} + Si_{RB} + Si_F + Si_{CB}} \times 100\% \quad (3)$$

that is, the overall content of SiC equals the SiC contents in each part of powders divided by the total powder; whereas the conversion of silicon equals the silicon in the form of SiC divided by the total silicon in the powders. Similarly, overall contents for free silicon and free carbon can also be calculated, the weighted average compositions of the total powder products and conversions of injected metallic silicon to SiC are given in Table IV.

EPMA, by means of X-ray energy dispersive spectroscopy (EDS) with an ultra-thin aluminium window was employed to determine the principal elements in the powder. One of the typical EDS spectra for filter powders (S8F) is shown in Fig. 10, together with the starting powder (Si-45), silicon powder evaporated in plasma (RFSi-1), and commercially available α-SiC powder for the purpose of comparison. As expected, the major peaks for silicon and carbon appear in the spectra. The presence of aluminium and iron originates from the source material. Gold and palladium were used to provide surface electrical conduction of the specimens by the sputtering technique. The peaks for aluminium and iron are found to be much stronger than they are in the spectra of the starting material, which was probably due to their relatively easy

TABLE III Characteristics of silicon carbide powders

Sample	Phase composition (wt %)				Ratio of α-SiC to β-SiC	SiC (wt %)	Specific surface area ($m^2 g^{-1}$)	Average diameter (nm)
	α-SiC	β-SiC	Si_f	C_f				
1RW	22.80	30.30	42.90	4.00	0.75	53.10	–	–
1CB	18.80	26.50	41.70	13.00	0.72	45.30	–	–
1F	46.36	52.88	0.25	0.50	0.88	99.25	43.8	43
5RW	16.36	26.08	52.57	5.00	0.63	42.44	10.0	187
5CB	13.30	23.84	47.86	15.00	0.56	37.14	18.7	100
5F	46.33	53.29	0.28	0.10	0.87	99.62	35.0	53
S2RW	28.65	38.25	29.10	4.00	0.75	66.90	24.8	75
S2CB	30.43	43.13	17.44	9.00	0.71	73.56	–	–
S2F	41.80	53.80	4.10	0.30	0.78	95.60	34.9	54
S8RW	35.79	47.94	10.47	5.80	0.75	83.73	27.0	69
S8CB	29.00	41.52	8.48	21.00	0.70	70.52	31.5	59
S8F	38.57	59.03	0.40	2.00	0.65	97.60	35.0	53
S15RW	35.82	53.70	8.29	2.20	0.67	89.52	30.1	62
S15CB	33.55	52.08	4.87	9.50	0.65	85.63	27.1	69
S15F	45.08	53.69	0.23	1.00	0.84	98.77	37.5	50

evaporation (the boiling points of aluminium and iron are 2790 and 3135 °C, respectively). It is noted that the peak for oxygen in the plasma-synthesized powders was weak, very similar to that for the commercial α-SiC (see Fig. 10d, for instance). This could be interesting because "SiO" was clearly observed in the micrograph of silicon powders obtained in the preliminary evaporation tests, mentioned in Section 4.1, and moreover, a strong peak for oxygen is observed in the EDS spectra of such powder (see Fig. 10b). EPMA for the powders collected at other positions produced similar spectra except for differences in the intensities of the peaks. The substantial reduction of oxygen content in the synthesized powders could be attributed to the production of free carbon with the injection of CH_4. It is very likely that some free carbon reacts with oxygen in the system and the produced CO and CO_2 escape from the system, together with the tail gas.

TABLE IV Overall conversion of metallic silicon to SiC

Run	Weighted average composition of collected powder (wt %)			Overall conversion of Si to SiC (%)
	SiC	Si_f	C_f	
1	50.77	44.81	4.42	44.2
5	40.79	54.07	5.14	34.6
S2	73.85	21.72	4.43	70.4
S8	84.77	7.65	7.58	88.6
S15	91.50	5.57	2.93	92.0

In order to examine further the existence of Si–O in the powder, infrared analysis was performed (FT–IR analysis). SiC powder of ~ 1 wt % was mixed with KBr by vibration. The FT–IR spectroscopy performed ranged from 600–4000 cm^{-1}. Fig. 11 shows the typical IR absorption spectrum of the SiC powder. The spectra of silicon powder evaporated in plasma (RFSi-1), which was partially oxidized as mentioned previously, and commercial α-SiC and β-SiC are also

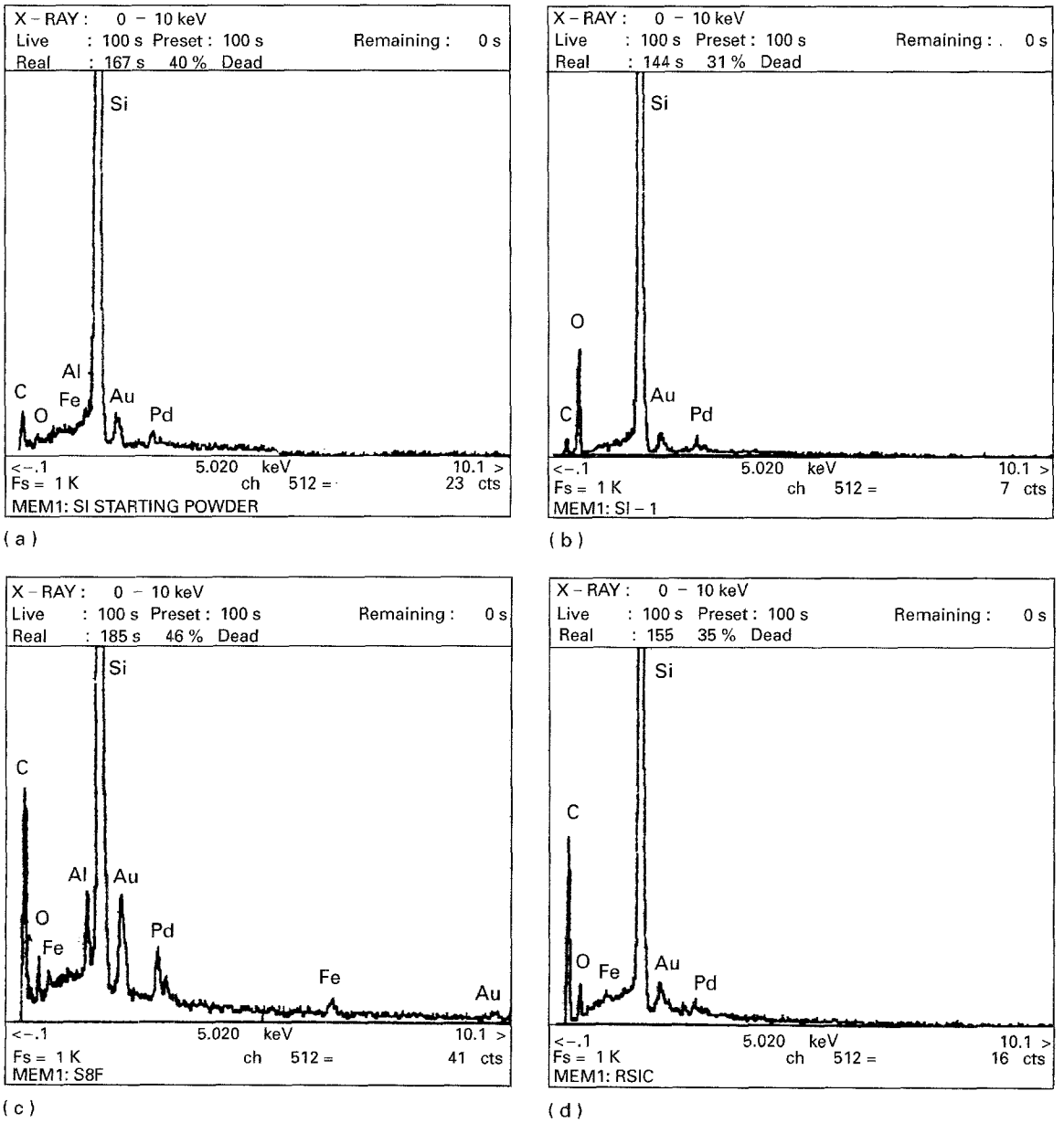

Figure 10 EDS spectra of different powders: (a) starting powder Si-45; (b) plasma-evaporated Si (RFSi-1); (c) plasma-synthesized SiC (S8F); (d) commercial α-SiC.

recorded for comparison purposes. It can be seen that the infrared absorption band for the Si–C bond is in the vicinity of 900 cm^{-1}. The absorption peak near 3500 cm^{-1} was due to water present in the KBr pellet or specimens and is thus assigned to the O–H stretching vibration. The presence of the absorption band at 2200 cm^{-1} may be assigned to a stretching vibration of the Si–H bond. The peak at around 1600 cm^{-1} was unable to be identified, although it is attributed elsewhere [28] to harmonics of SiC bulk. It should be noted that the characteristic absorption band in the region of ~ 800 and 1100 cm^{-1} for Si–O bond stretching vibration is not visible, implying that the oxygen content in the powder is at an equivalent level to that of commercially available SiC powders. The i.r. result is consistent with the EPMA. A previous study [29] indicated that oxygen in ultrafine SiC powders was present primarily in the form of adsorption on the surface of the powders. It is well known that as ultrafine non-oxide powders such as SiC and Si_3N_4 are exposed to air for extended periods of time, the oxygen content of the powders increases substantially.

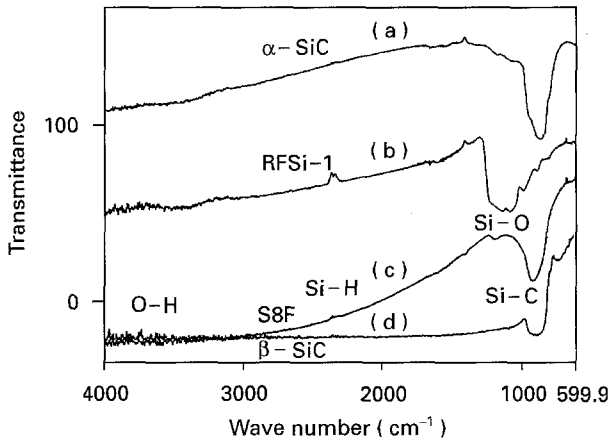

Figure 11 IR spectroscopy of different powders: (a) commercial α-SiC; (b) plasma-treated Si (RFSi-1); (c) plasma-synthesized SiC (S8F); (d) commercial β-SiC.

The surface areas of the pure SiC powders, as measured by the BET method, range from 35–50 $m^2 g^{-1}$. When this result is combined with the TEM observations, the average particle size can be estimated and it is found to be in the range 40–80 nm. Fig. 12 shows the transmission electron micrograph for SiC ultrafine powder. The particles are basically equiaxed. The free carbon surrounding the SiC particles is visible in some of the micrographs.

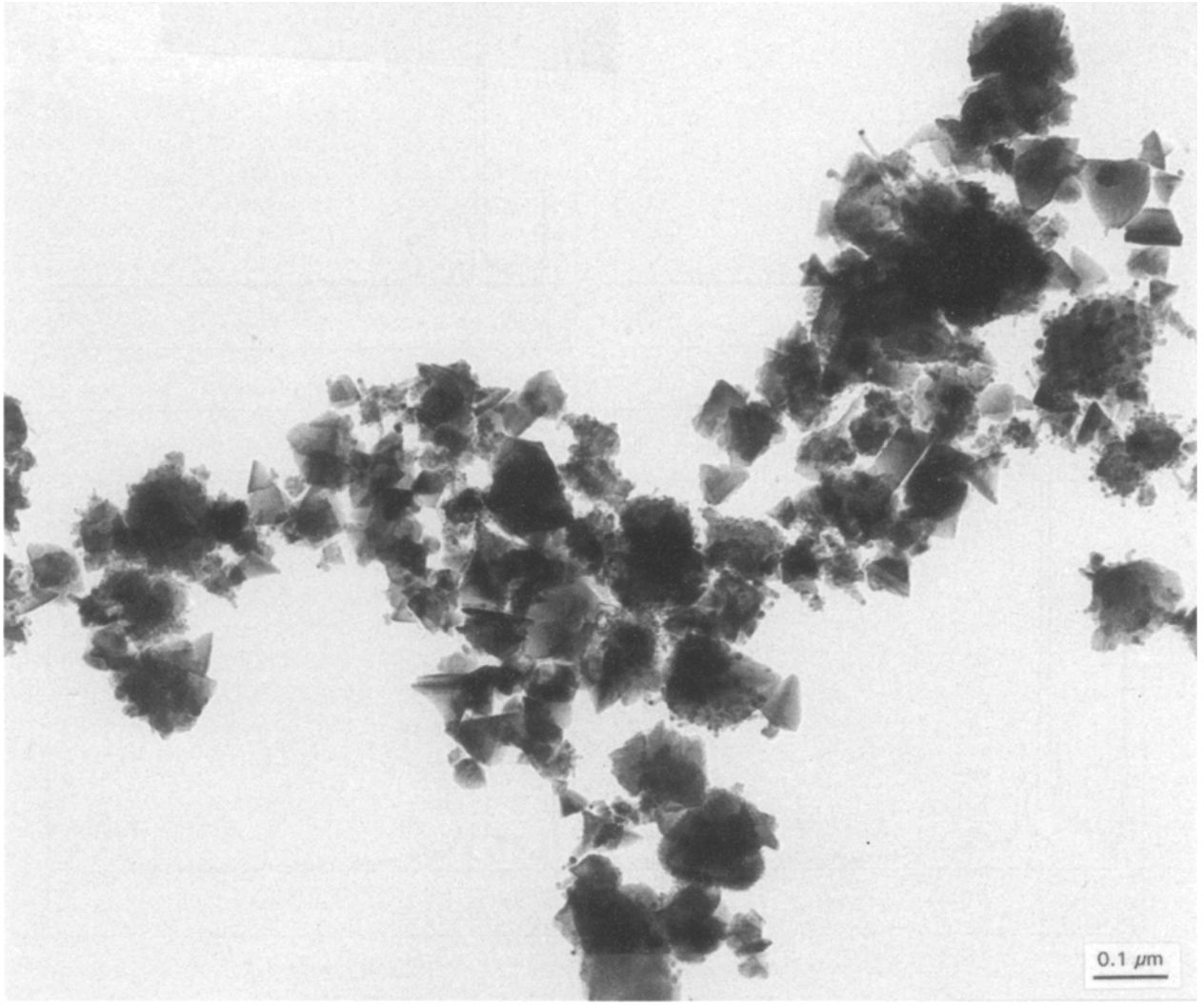

Figure 12 Transmission electron micrograph of ultrafine SiC powder.

5. Conclusion

Ultrafine SiC powder (40–80 nm) was synthesized by the reaction of introduced metallic silicon powder and methane in an induction plasma reactor. Purity levels of up to 98 wt % SiC were observed in the filter-collected powder. The powders collected from other system parts were found to be mixtures of silicon carbide, spheroidized silicon, unreacted free silicon and free carbon. The overall content of SiC in the total collected powder and the conversion of metallic silicon to SiC reached 91.5 wt % and 92.0%, respectively, for the case of Si-45 used as starting material and appropriate selection of the experimental parameters. The formation of SiC relies on the evaporation of the injected metallic silicon, which in turn is mainly dependent on the particle size of the starting silicon powder.

Acknowledgements

The authors gratefully acknowledge the financial support of the Conseil de Recherche en Sciences Naturelle et en Genie du Canada (CRSNG) and the scholarship of the Canadian International Development Agency (CIDA). We also appreciate Dr Peter Lanigan's contribution for his effort in the proof-reading of this paper.

References

1. C. M. HOLLABAUGH, D. E. HULL, L. R. NEWKIRK and J. J. PETROVIC, *J. Mater. Sci.* **18** (1983) 3190.
2. G. J. VOGT, R. S. VIGIL, L. R. NEWKIRK and M. TRKULA, in Proceedings of the 7th International Symposium on Plasma Chemistry, Eindhoven, The Netherlands, July 1985, edited by C. J. Timmermans (IUPAC, Eindhoven, 1985) pp. 668–73.
3. Y. SUYAMA, R. M. MARRA, J. S. HAGGERTY and H. K. BOWEN, *Am. Ceram. Soc. Bull.* **64** (1985) 1356.
4. M. V. HOESSLIN , R. KOCH, J. H. SCHAFER, J. UHLENBUSCH and W. VIOL in Proceedings of 9th International Symposium on Plasma Chemistry, Pugnochiuso, Italy, September 1989, edited by R. d'Agostino (IUPAS, 1989) p. 854.
5. L. CHEN, T. GOTO and T. HIRAI, *J. Mater. Sci.* **24** (1989) 3824.
6. R. M. SALINGER, *Ind. Eng. Chem. Prod. Res. Develop.* **11** (1972) 230.
7. J. Y. GUO and G. L. ZHENG, *Eng. Chem. Metall.* **12** (1991) 1.
8. M. ENDO, T. SANO, N. URASATO and M. SHIRAISHI, *Yogyo-Kyokai-Shi* (Jpn), **95** (1987) 104.
9. A. MITSUI and A. KATO, *Yogyo Kyokaishi* **94** (1986) 517.
10. T. KAMEYAMA, K. SAKANAKA, A. MOTOE, T. TSUNODA, T. NAKANAGA, N. I. WAKAYAMA, H. TAKEO and K. FUKUDA, *J. Mater. Sci.* **25** (1990) 1058.
11. H. J. LEE , K. EQUCHI and T. YOSHIDA, *J. Am. Ceram. Soc.* **73** (1990) 3356.
12. H. R. BAUMAGARTNER and B. R. ROSSING, in "Ceramic Transaction", Vol. 2, "Silicon Carbide '87", edited by J. D. Cawley and C. E. Semler (American Ceramic Society, Westerville, OH, 1989) pp. 3–16.
13. P. H. RIETH, J. S. REED and A. W. NAUMANN, *Am. Ceram. Soc. Bull.* **55** (1976) 713.
14. G. C. WEI, *Am. Ceram. Soc.* **66** (1983) C111.
15. K. M. RIGTRUP and R. A. CUTLER, in "Silicon Carbide '87", "Ceramic Transaction", Vol. 2 edited by J. D. Cawley and C. E. Semler (American Ceramic Society, Westerville, OH, 1989) pp. 17–33.
16. O. YAMADA, Y. MIYAMOTO and M. KOIZUMI, *J. Mater. Res.* **1** (1986) 275.
17. Y. ANDO, M. OHKOHCHI and R. UYEDA, *Jpn J. Appl. Phys.* **19** (1980) L693.
18. P. C. KONG, T. T. HUANG and E. PFENDER, in Proceedings of the International Symposium on Plasma Chemistry, Montreal, Canada, July 1983, edited by M. I. Boulos and R. J. Wlunz (IUPC, 1983) pp. 219–224.
19. P. KONG, R. M. YOUNG, T. T. HUANG and E. PFENDER, in Proceedings of the 7th International Symposium on Plasma Chemistry Eindhoven, The Netherlands, July 1985, edited by C. J. Timmermans (IUPAC, Eindhoven, 1985) pp. 674–9.
20. K. TANAKA, K. ISHIZAKI, S. YUMOTO, T. EGASHIRA and M. UDA, *J. Mater. Sci.* **22** (1987) 2192.
21. K. ISHIZAKI, S. YUMOTO and K. TANAKA, *J. Mater. Sci.* **23** (1988) 1813.
22. Y. INOUE, Y. NARIKI and K. TANAKA, *J. Mater. Sci.* **24** (1989) 3819.
23. C. B. LAFLAMME, Doctoral thesis, University of Sherbrooke, August 1991.
24. C. R. VEALE, "Fine powders-preparation, properties and uses" (Halsted Press, Wiley, New York, 1972) p. 42.
25. P. PROULX, J. T. MOSTAGHIMI and M. I. BOULOS, *Int. J. Heat Mass Transfer* **28** (1985) 1327.
26. *Idem, Plasma Chem. Plasma Process.* **7** (1987).
27. J. G. SHEEK and J. D. CAWLEY, in "Ceramic Transaction", Vol. 2 "Silicon Carbide '87", edited by J. D. Cawley and C. E. Semler (American Ceramic Society, Westerville, OH, 1989) pp. 47–61.
28. G. RAMIS , P. QUINTARD, M. CAUCHETIER, G. BUSCA and V. LORENZELLI, *J. Am. Ceram. Soc.* **72** (1989) 1692.
29. G. L. ZHENG and J. Y. GUO, in Proceedings of 8th International Symposium on Plasma Chemistry, Tokyo, Japan, August 1987, edited by K. Akashi and A. Kinbara (IUPAC, 1987) p. 2081.

Received 4 January
and accepted 5 April 1995